CERN-EP-2021-179
25 August 2021

Observation of the suppressed $\Lambda_b^0 \rightarrow DpK^-$ decay with $D \rightarrow K^+\pi^-$ and measurement of its *CP* asymmetry

LHCb collaboration[†]

Abstract

A study of Λ_b^0 baryon decays to the DpK^- final state is presented based on a proton-proton collision data sample corresponding to an integrated luminosity of 9 fb^{-1} collected with the LHCb detector. Two Λ_b^0 decays are considered, $\Lambda_b^0 \rightarrow DpK^-$ with $D \rightarrow K^-\pi^+$ and $D \rightarrow K^+\pi^-$, where D represents a superposition of D^0 and \bar{D}^0 states. The latter process is expected to be suppressed relative to the former, and is observed for the first time. The ratio of branching fractions of the two decays is measured, and the *CP* asymmetry of the suppressed mode, which is sensitive to the CKM angle γ , is also reported.

Submitted to Phys. Rev. D

© 2021 CERN for the benefit of the LHCb collaboration. CC BY 4.0 licence.

[†]Authors are listed at the end of this paper.

1 Introduction

Beauty-baryon decays to final states involving a single open-charm meson are little studied but are promising for measurements of CP violation. A measurement of a set of branching fraction ratios of Λ_b^0 and Ξ_b decays to final states including a D meson yielded the first observation of the singly-Cabibbo-suppressed $\Lambda_b^0 \rightarrow [K^-\pi^+]_D p K^-$ decay [1], where D represents a D^0 or \bar{D}^0 meson.¹ This was followed by a study of the resonant structure of $\Lambda_b^0 \rightarrow D^0 p \pi^-$ decays [2].

This paper reports the results of a study of $\Lambda_b^0 \rightarrow D p K^-$ decays with the objectives of observing for the first time the $\Lambda_b^0 \rightarrow D p K^-$ decay with $D \rightarrow K^+\pi^-$, denoted as $\Lambda_b^0 \rightarrow [K^+\pi^-]_D p K^-$ and measuring its CP asymmetry. This decay is expected to be suppressed relative to the $\Lambda_b^0 \rightarrow [K^-\pi^+]_D p K^-$ decay. An estimate of the ratio of branching fractions between the favoured and suppressed modes is obtained by considering the relevant Cabibbo-Kobayashi-Maskawa (CKM) matrix elements

$$R \approx \left| \frac{V_{cb} V_{us}^*}{V_{ub} V_{cs}^*} \right|^2 = 7.4. \quad (1)$$

The $\Lambda_b^0 \rightarrow [K^-\pi^+]_D p K^-$ ($\Lambda_b^0 \rightarrow [K^+\pi^-]_D p K^-$) decay with same (opposite) sign kaons are referred to as the favoured (suppressed) decay throughout this paper. The suppressed decay is of particular interest since its decay amplitude receives contributions from $b \rightarrow c$ and $b \rightarrow u$ amplitudes of similar magnitude, given the CKM suppression between the two D decays. The interference between these two amplitudes, which depends upon the CKM angle γ , is expected to be large [3, 4], but the different strong phases associated with the various configurations of polarisation states for the Λ_b^0 , proton, and intermediate resonances complicate determination of γ .

The analysis is based on proton-proton (pp) collision data collected with the LHCb detector at $\sqrt{s} = 7, 8, \text{ and } 13$ TeV, corresponding to a total integrated luminosity of 9 fb^{-1} . The suppressed $\Lambda_b^0 \rightarrow [K^+\pi^-]_D p K^-$ decay is observed for the first time. In addition the ratio of branching fractions of the favoured and suppressed decays, R , and the CP asymmetry in the suppressed mode, A , which is expected to be sensitive to the CKM angle γ , are measured where

$$R = \frac{\mathcal{B}(\Lambda_b^0 \rightarrow [K^-\pi^+]_D p K^-)}{\mathcal{B}(\Lambda_b^0 \rightarrow [K^+\pi^-]_D p K^-)},$$

including both flavours, and

$$A = \frac{\mathcal{B}(\Lambda_b^0 \rightarrow [K^+\pi^-]_D p K^-) - \mathcal{B}(\bar{\Lambda}_b^0 \rightarrow [K^-\pi^+]_D \bar{p} K^+)}{\mathcal{B}(\Lambda_b^0 \rightarrow [K^+\pi^-]_D p K^-) + \mathcal{B}(\bar{\Lambda}_b^0 \rightarrow [K^-\pi^+]_D \bar{p} K^+)}. \quad (2)$$

Sensitivity to CP -violation requires interference between amplitudes involving intermediate D^0 and \bar{D}^0 mesons. This interference is anticipated to be amplified in regions of the phase space involving $\Lambda_b^0 \rightarrow DX$ contributions, where X labels excited Λ states. Therefore, the ratio of branching fractions and the CP asymmetry in the suppressed mode are measured separately in the full phase space and in a reduced phase-space region which involves $\Lambda_b^0 \rightarrow DX$ decays, where an enhanced sensitivity to γ is expected.

¹Charge conjugation is implied throughout this document except in reference to CP asymmetries or comparisons of Λ_b^0 and $\bar{\Lambda}_b^0$ samples.

2 Detector and simulation

The LHCb detector [5,6] is a single-arm forward spectrometer covering the pseudorapidity range $2 < \eta < 5$, designed for the study of particles containing b or c quarks. The detector includes a high-precision tracking system consisting of a silicon-strip vertex detector surrounding the pp interaction region [7], a large-area silicon-strip detector located upstream of a dipole magnet with a bending power of about 4 Tm, and three stations of silicon-strip detectors and straw drift tubes [8,9] placed downstream of the magnet. The tracking system provides a measurement of the momentum, p , of charged particles with a relative uncertainty that varies from 0.5% at low momentum to 1.0% at 200 GeV/ c . The minimum distance of a track to a primary pp collision vertex (PV), the impact parameter (IP), is measured with a resolution of $(15 + 29/p_T) \mu\text{m}$, where p_T is the component of the momentum transverse to the beam, in GeV/ c . Different types of charged hadrons are distinguished using information from two ring-imaging Cherenkov detectors [10]. Hadrons are identified by a calorimeter system consisting of scintillating-pad and preshower detectors, an electromagnetic and a hadronic calorimeter. The online event selection is performed by a trigger [11], which consists of a hardware stage, based on information from the calorimeter, followed by a software stage, which applies a full event reconstruction.

Simulation is required to model the effects of the detector acceptance and the imposed selection requirements. In the simulation, pp collisions are generated using PYTHIA [12] with a specific LHCb configuration [13]. Decays of unstable particles are described by EVTGEN [14], in which final-state radiation is generated using PHOTOS [15]. The interaction of the generated particles with the detector, and its response, are implemented using the GEANT4 toolkit [16] as described in Ref. [17].

The particle identification (PID) response in the simulated samples is corrected using control samples of $\Lambda_c^+ \rightarrow pK^-\pi^+$ decays in LHCb data, taking into account its correlation with the kinematic properties of each track and with the event multiplicity. To parametrise the PID response, an unbinned method is employed, where the probability density functions (PDFs) are modelled using kernel density estimation [18].

3 Reconstruction and selection of candidates

Neutral D meson candidates are reconstructed by combining kaon and pion candidates having opposite charge. To form Λ_b^0 candidates, the neutral D meson candidates are combined with proton and kaon candidates having opposite charge. Each Λ_b^0 candidate is associated to the PV for which the value of χ_{IP}^2 is minimised, where χ_{IP}^2 is the difference between the vertex χ^2 of a given PV with and without the Λ_b^0 candidate included in the PV fit. The tracks forming the Λ_b^0 candidate and the beauty and charm vertices are required to have good fit quality and to be well separated from any PV in the event. The invariant masses of the Λ_b^0 candidate, $M(DpK^-)$, and of the D candidate, $M(K\pi)$, are required to be in the intervals from 5200 to 7000 MeV/ c^2 and 1850 to 1880 MeV/ c^2 , respectively. Candidates with $M(K\pi)$ in a wider mass range from 1765 to 1965 MeV/ c^2 are retained to quantify the background contribution from charmless b -hadron decays. A kinematic fit is performed in which $M(K\pi)$ is constrained to the known D^0 mass [19] and the Λ_b^0 candidate's trajectory is required to point back to the associated PV [20]. To improve the

resolution of the squared invariant masses $M^2(Dp)$, $M^2(DK^-)$ and $M^2(pK^-)$, the fit is repeated with the additional constraint that the invariant mass of the DpK^- combination is equal to the known Λ_b^0 mass [19] is applied when calculating these variables. Inclusion of the mass constraint improves the resolution on the two-body masses by 50% or more, depending upon position in the three-body phase space.

Background from $\Lambda_b^0 \rightarrow \Lambda_c^+ h^-$ decays, with $\Lambda_c^+ \rightarrow ph^- h^+$ where h is a charged kaon or pion, are vetoed by requiring that the invariant mass of any $ph^- h^+$ combination differs from the known Λ_c^+ mass [19] by more than $20 \text{ MeV}/c^2$. To suppress the contribution of events from charmless $\Lambda_b^0 \rightarrow ph^- h^+ h^-$ decays, the decay-time significance of the D meson candidates with respect to the Λ_b^0 vertex is required to be larger than 2.5. The decay-time significance of the D candidate is defined as the measured decay time divided by its uncertainty.

To suppress combinatorial background, a Boosted Decision Tree (BDT) algorithm using adaptive boosting [21] is employed as implemented in the TMVA toolkit [22]. To train the BDT classifier, one for the full and another for the restricted phase space, a sample of simulated $\Lambda_b^0 \rightarrow [K^- \pi^+]_D p K^-$ decays is used as a proxy for signal and candidates in the Λ_b^0 mass sidebands with mass in the intervals from 5300 to 5400 MeV/c^2 and from 5900 to 6000 MeV/c^2 are used to represent combinatorial background. The variables that enter the BDT selection are the quality of the kinematic fit, the quality of the Λ_b^0 and D vertices and their decay-time significances, PID variables, and the p_T of the final-state particles. The optimisation criterion used to determine the choice of BDT working point is the maximum expected statistical significance of the suppressed signal, $N_{\text{sig}}/\sqrt{N_{\text{sig}} + N_{\text{bkg}}}$, where N_{sig} and N_{bkg} are the expected numbers of signal and background candidates in the mass interval from 5600 to 5640 MeV/c^2 . The expected number of signal decays is determined by dividing the observed yield in the favoured decay by the Cabibbo suppression factor of 7.4 estimated in Eq. 1. In 0.1% of events multiple Λ_b^0 candidates are reconstructed. All the candidates are retained.

4 Determination of signal yields

The mass distributions for the DpK^- candidates in the favoured and suppressed data samples in the full phase space are shown in Fig. 1. The number of signal candidates is obtained by an extended unbinned maximum-likelihood fit to the $M(DpK^-)$ mass distributions using the ROOFIT package [23]. The favoured and suppressed samples are fitted simultaneously. The PDF used for the favoured sample is made of two components to model $\Lambda_b^0 \rightarrow DpK^-$ and $\Xi_b^0 \rightarrow DpK^-$ signals, a background from misidentified $\Lambda_b^0 \rightarrow Dp\pi^-$ decays, and a partially reconstructed background from $\Lambda_b^0 \rightarrow D^* p K^-$ decays where $D^{*0} \rightarrow D^0 \gamma$ or $D^{*0} \rightarrow D^0 \pi^0$ and the γ or π^0 particle is not reconstructed. Additional components are required to describe the background due to partially reconstructed $\Lambda_b^0 \rightarrow D^* p \pi^-$ decays, with $D^{*0} \rightarrow D^0 \gamma$ or $D^{*0} \rightarrow D^0 \pi^0$ and having the pion from the Λ_b^0 decay misidentified as a kaon, partially reconstructed $\Xi_b^0 \rightarrow D^* p K^-$ decays, which peak in the signal region, and from combinatorial background. The PDF used to fit the suppressed sample is the same, except that it does not include contributions from the $\Xi_b^0 \rightarrow D^{(*)} p K^-$ and $\Lambda_b^0 \rightarrow D^{(*)} p \pi^-$ decays, which are expected to be negligible.

The parametrised shape of each component is taken from a fit to simulated decays after all selections are applied. The signal and partially reconstructed background are

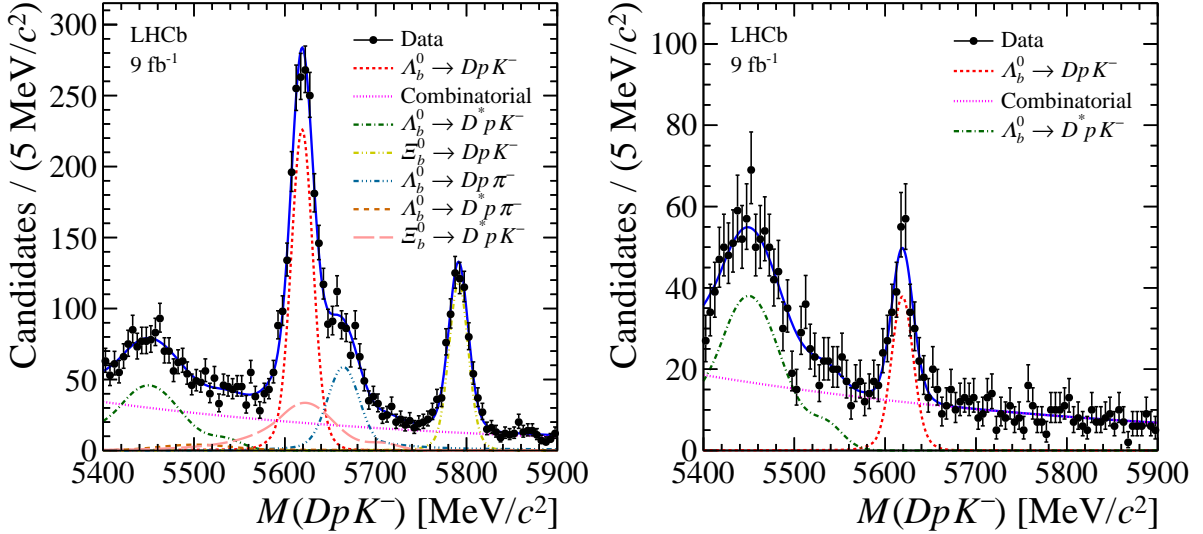


Figure 1: Distributions of the invariant mass for selected (left) $\Lambda_b^0 \rightarrow [K^-\pi^+]DpK^-$ and (right) $\Lambda_b^0 \rightarrow [K^+\pi^-]DpK^-$ candidates in the full phase space (black points). The total fit model, as described in the text, is indicated by the solid blue line, and individual components are indicated.

each modelled by the sum of two Crystal Ball (CB) functions [24], where the parameters governing the shape of the tails are fixed to their values in fits to simulated samples. The background from misidentified $\Lambda_b^0 \rightarrow Dp\pi^-$ decays is parametrised by the sum of a Gaussian and a CB function. In the restricted phase-space region, $M^2(pK^-) < 5 \text{ GeV}^2/c^4$, the same functional forms are used, except that the partially reconstructed background is parametrised by the sum of a bifurcated Gaussian and a CB function. The combinatorial background is described by an exponential function. The slope of the combinatorial background is allowed to vary independently in the favoured and suppressed samples. The widths of each peaking component are multiplied by a common free parameter in order to account for the difference between the invariant-mass resolution observed in data and simulation. The mass of the Λ_b^0 baryon is a free parameter, while the mass difference between Ξ_b^0 and Λ_b^0 baryons is fixed to its known value [19]. The yields of each component are allowed to vary independently in the favoured and suppressed samples.

The projection of the fit to the invariant-mass distribution $M(DpK^-)$ in the favoured and suppressed data samples in the full phase space is shown in Fig. 1. The Λ_b^0 yields are 1437 ± 92 for the favoured mode and 241 ± 22 for the suppressed mode. Figure 2 shows the invariant-mass distribution $M(DpK^-)$ in the favoured and suppressed data samples in the restricted phase-space region $M^2(pK^-) < 5 \text{ GeV}^2/c^4$ with the fit projections overlaid. In this fit, the Λ_b^0 yields are 664 ± 36 and 84 ± 14 for the favoured and suppressed modes, respectively. The invariant-mass distributions $M(DpK^-)$ and $M(D\bar{p}K^+)$, overlaid with the fit projections, used to calculate the CP asymmetry of the suppressed decay in the full phase space and in the restricted phase-space region are shown in Figs. 3 and 4, respectively.

The resonant structure of the favoured and suppressed decays can be illuminated by considering projections of the Λ_b^0 phase space. Figure 5 shows the $M^2(pK^-)$ and $M^2(Dp)$ distributions of favoured and suppressed candidates in the signal region $5600 <$

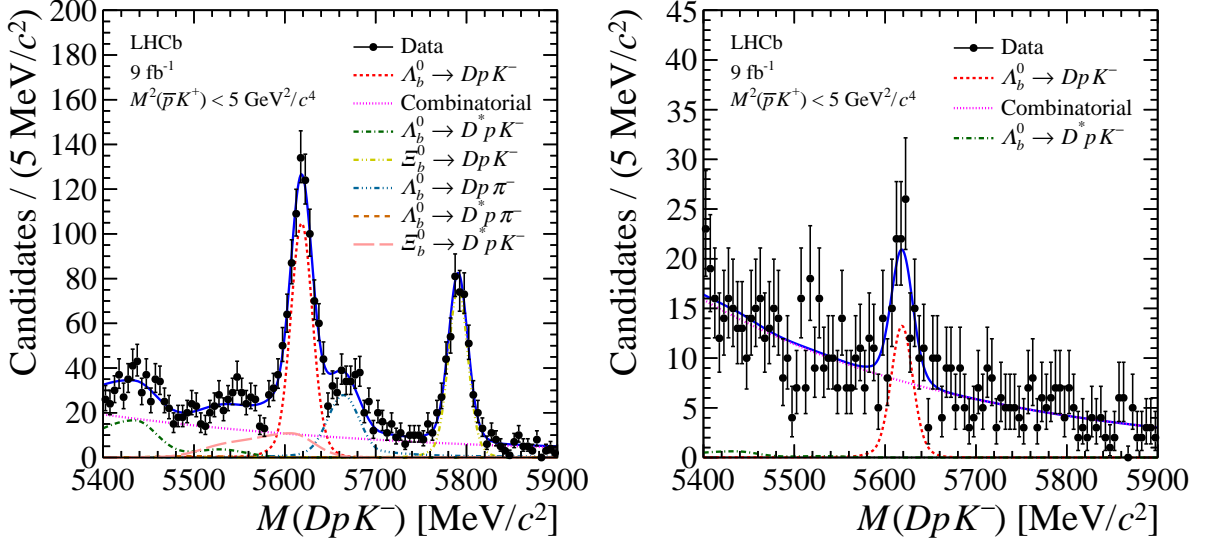


Figure 2: Distributions of the invariant mass for (left) $\Lambda_b^0 \rightarrow [K^- \pi^+]_{Dp} K^-$ and (right) $\Lambda_b^0 \rightarrow [K^+ \pi^-]_{Dp} K^-$ candidates in the restricted phase-space region $M^2(pK^-) < 5 \text{ GeV}^2/c^4$. The fit, as described in the text, is overlaid.

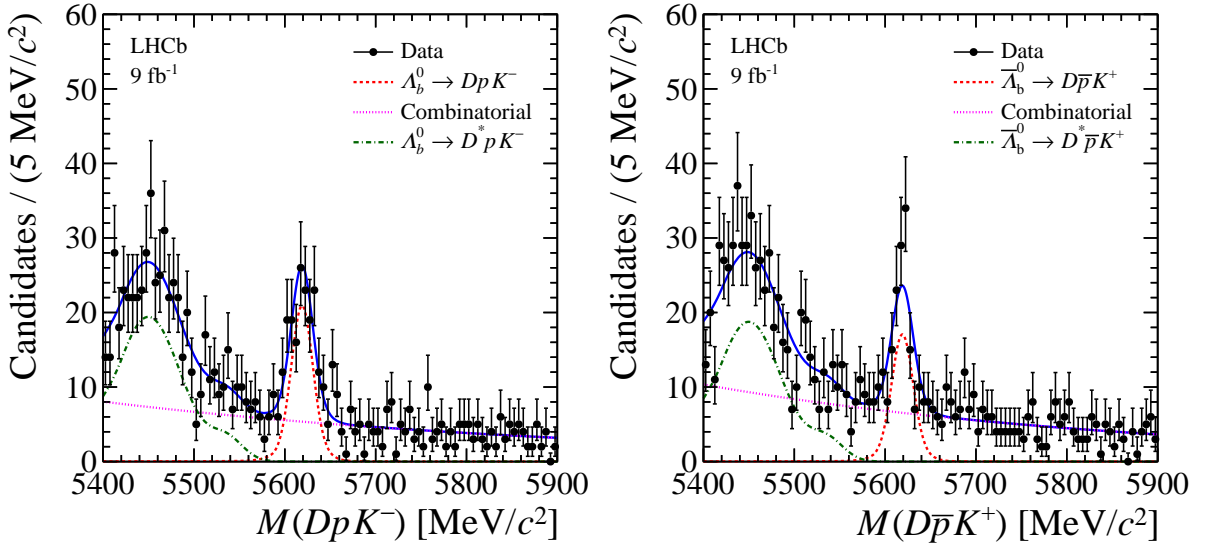


Figure 3: Distributions of the invariant mass for (left) $\Lambda_b^0 \rightarrow [K^+ \pi^-]_{Dp} K^-$ and (right) $\bar{\Lambda}_b^0 \rightarrow [K^- \pi^+]_{D\bar{p}} K^+$ candidates in the full phase space (black points). The fit, as described in the text, is indicated by the solid blue line, and individual components are indicated.

$M(DpK^-) < 5640 \text{ MeV}/c^2$. The signal purity in this region is 76% and 72% for the favoured and suppressed modes, respectively. Despite the smaller combinatorial background, the signal purity for the favoured decay is comparable to that for the suppressed decay due to the presence of the background from $\Xi_b^0 \rightarrow D^* p K^-$ and $\Lambda_b^0 \rightarrow D p \pi^-$ decays in the signal region. Figures 6 and 7 show invariant-mass projections onto $M(pK^-)$, $M(Dp)$ and $M(DK^-)$ for selected candidates. The dominant resonant amplitudes in the favoured

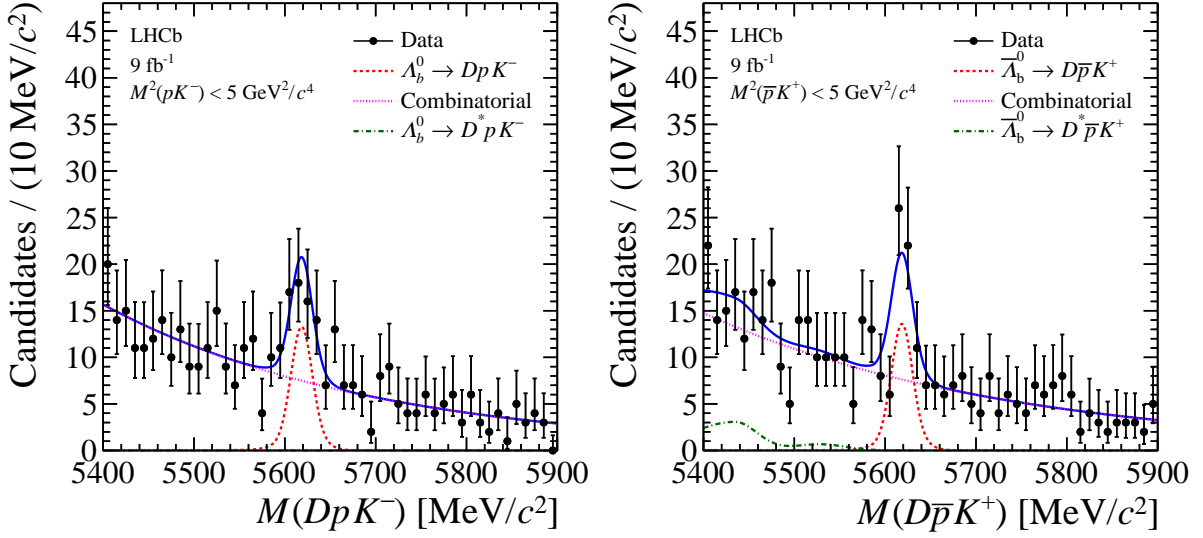


Figure 4: Distributions of the invariant mass for (left) $\Lambda_b^0 \rightarrow [K^+\pi^-]_D p K^-$ and (right) $\bar{\Lambda}_b^0 \rightarrow [K^-\pi^+]_D \bar{p} K^+$ candidates in the restricted phase-space region (black points). The fit, as described in the text, is indicated by the solid blue line, and individual components are indicated.

mode could generate structures in the $M(Dp)$ and $M(pK^-)$ distributions, corresponding to states having udc and uds quark content, respectively. The $M(Dp)$ distribution shows an increased density of events in the low- $M(Dp)$ region with a contribution from $\Lambda_c(2860)^+ \rightarrow D^0 p$ decays. The distribution of $M(pK^-)$ contains a contribution from the $\Lambda(1520)$ baryon at low- $M(pK^-)$ and an enhancement at $2.5 \lesssim M(pK^-) \lesssim 3.5 \text{ GeV}/c^2$, which is the reflection of the $\Lambda_c(2860)^+$ resonance seen in the $M(Dp)$ distribution. Different resonant structure is anticipated in the suppressed sample given the contributions from, and interference between, the $\Lambda_b^0 \rightarrow D^0 p K^-$ and $\Lambda_b^0 \rightarrow \bar{D}^0 p K^-$ amplitudes. The $M(DK^-)$ distribution in the suppressed sample shows an increased density of events in the low-mass region with a contribution from resonances decaying to DK^- such as the $D_{s1}^*(2700)^\pm$.

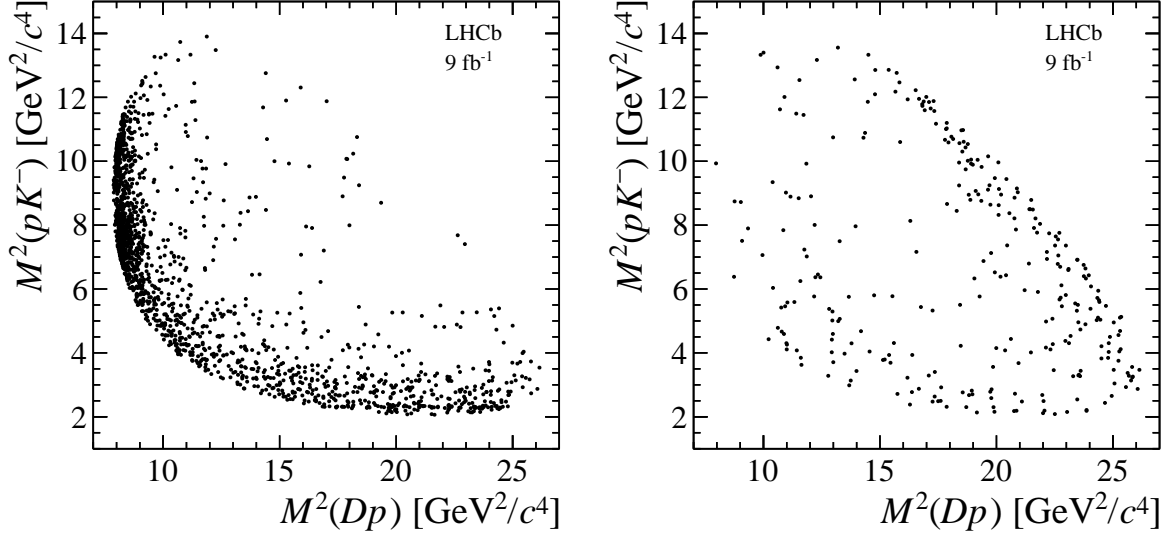


Figure 5: Phase space of the (left) $\Lambda_b^0 \rightarrow [K^- \pi^+] Dp K^-$ and (right) $\Lambda_b^0 \rightarrow [K^+ \pi^-] Dp K^-$ candidates having a mass between 5600 and 5640 MeV/c^2 . No background subtraction is applied.

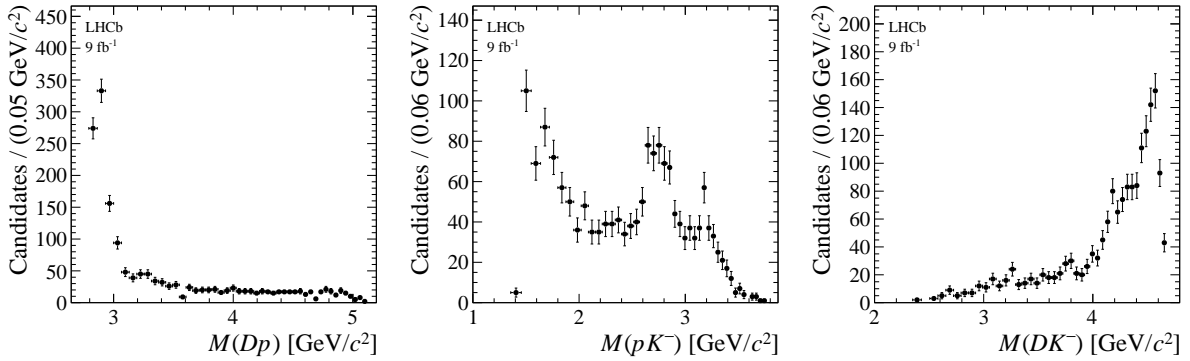


Figure 6: Invariant-mass projections of the Λ_b^0 phase space in (left) $M(Dp)$, (middle) $M(pK^-)$, and (right) $M(DK^-)$ for the $\Lambda_b^0 \rightarrow [K^- \pi^+] Dp K^-$ candidates.

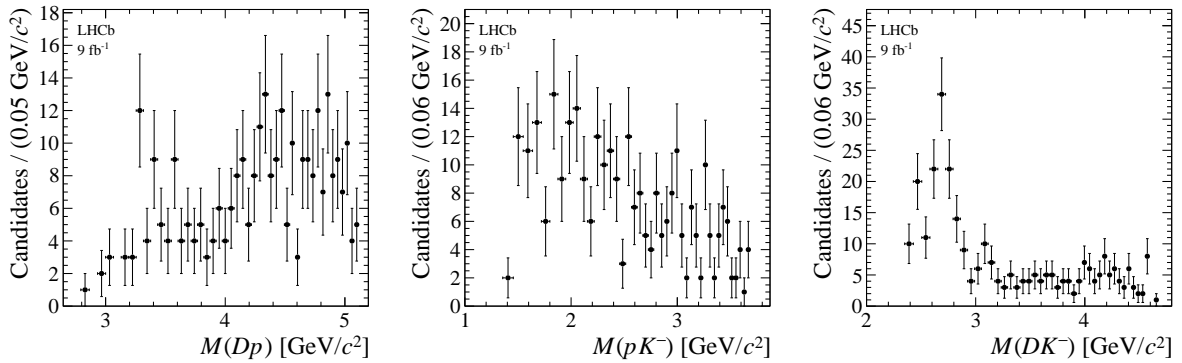


Figure 7: Invariant-mass projections of the Λ_b^0 phase space in (left) $M(Dp)$, (middle) $M(pK^-)$, and (right) $M(DK^-)$ for the $\Lambda_b^0 \rightarrow [K^+ \pi^-] Dp K^-$ candidates.

5 Calculation of branching fraction ratio and CP asymmetry

The ratio of branching fractions of the favoured and suppressed decays and the CP asymmetry of the suppressed decay are calculated from the ratio of yields of the corresponding decays after applying efficiency correction factors as

$$R = \frac{\sum_i w_{\text{FAV}}^i / \epsilon^i}{\sum_i w_{\text{SUP}}^i / \epsilon^i}, \quad (3)$$

$$A = \frac{\sum_i w_{\text{SUP}, \Lambda_b^0}^i / \epsilon^i - \sum_i w_{\text{SUP}, \bar{\Lambda}_b^0}^i / \epsilon^i}{\sum_i w_{\text{SUP}, \Lambda_b^0}^i / \epsilon^i + \sum_i w_{\text{SUP}, \bar{\Lambda}_b^0}^i / \epsilon^i} \quad (4)$$

where the sum is over the selected candidates. Here w_{FAV}^i and w_{SUP}^i are the weights obtained using the *sPlot* technique [25] for background subtraction of the favoured or suppressed samples, respectively, with $M(DpK^-)$ as the discriminating variable. The subscripts Λ_b^0 and $\bar{\Lambda}_b^0$ label the samples split by flavour and ϵ^i are the relative efficiencies. The efficiency corrections are determined as a function of the Λ_b^0 phase-space variables $M^2(Dp)$ and $M^2(pK^-)$ using the simulated $\Lambda_b^0 \rightarrow [K^- \pi^+]_D p K^-$ sample and parameterised by a kernel density estimation technique [18]. Across the phase space, the relative efficiencies vary from 0.7 to 1.2, as shown in Figure 8.

The measured values of R and A in the full phase space with their statistical and

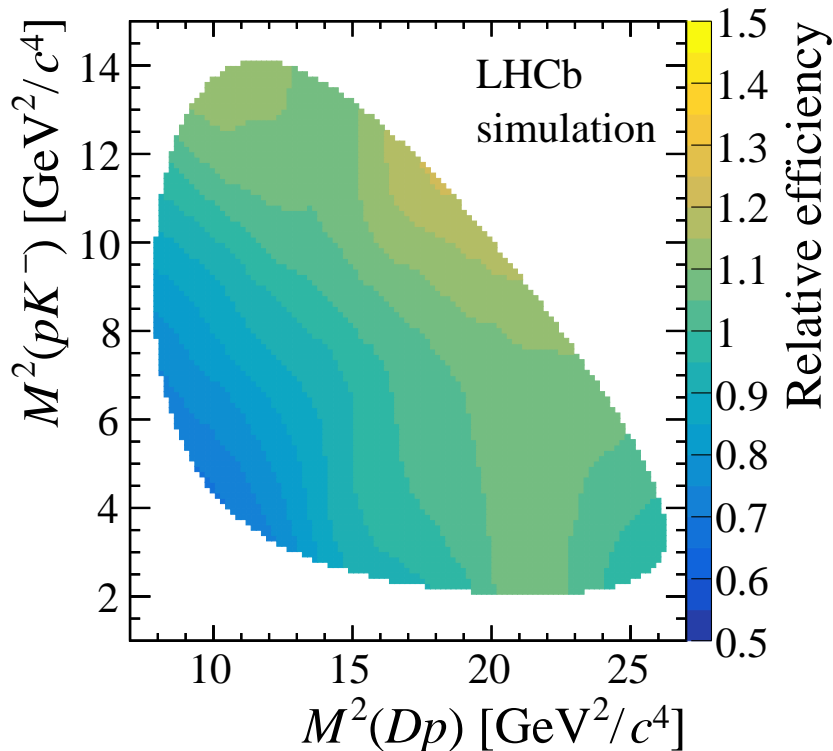


Figure 8: Relative efficiency correction as a function of position within the Λ_b^0 phase space, obtained from simulated samples.

systematic uncertainties are

$$R = 7.1 \pm 0.8 \text{ (stat.)}_{-0.3}^{+0.4} \text{ (syst.)},$$

$$A = 0.12 \pm 0.09 \text{ (stat.)}_{-0.03}^{+0.02} \text{ (syst.)},$$

and in the phase-space region $M^2(pK^-) < 5 \text{ GeV}^2/c^4$,

$$R = 8.6 \pm 1.5 \text{ (stat.)}_{-0.3}^{+0.4} \text{ (syst.)},$$

$$A = 0.01 \pm 0.16 \text{ (stat.)}_{-0.02}^{+0.03} \text{ (syst.)}.$$

The data samples in the full and restricted phase-space region partially overlap and the statistical uncertainties on the ratios and asymmetries measured in these two regions are correlated. A positive correlation between the statistical uncertainties of $\rho = 0.33$ is estimated, given the number of events in the two samples and their overlap.

6 Systematic uncertainties

The systematic uncertainties on the ratio of branching fractions of the favoured and suppressed decays and the CP asymmetry of the suppressed decay are listed in Table 1. For each variation, the determination of R and A is performed, and the difference with respect to the nominal result is taken as systematic uncertainty. Where multiple variations are considered, the largest negative and positive deviations are taken. For the measurement of R and A , many systematic effects cancel in the ratios. The total systematic uncertainties are obtained by summing all the contributions in quadrature.

To assess systematic uncertainties due to the description of signal and background contributions in the invariant mass fit model, alternative parameterisations for the Λ_b^0 mass peak, partially reconstructed background components and combinatorial background are used. The corresponding systematic uncertainties amount to (1–5)%. The efficiency corrections are impacted by the limited size of the signal simulation sample. This is assessed by varying the parameters of the kernel density estimation. The corresponding systematic uncertainties are (1–3)%.

The PID response in data is obtained from calibration samples [26, 27]. The associated systematic uncertainty includes the kernel width variation and the uncertainty due to finite sample size of the calibration samples. The resulting uncertainty is 2% for R , and less than 1% for A .

The hardware-level trigger decision is not perfectly simulated. The impact of this mismodelling is estimated by varying the efficiency map according to a correction obtained from data control samples. The resulting systematic uncertainty is at the level of 0.5%.

The background from charmless decays is estimated by interpolating from the D mass sidebands into the D mass region after all selection requirements are imposed and found to be 0.5% and 1% in the favoured and suppressed samples, respectively. These values are taken as uncertainties and propagated to the measurement of R , resulting in an uncertainty of 1% on R , while the corresponding uncertainty on A is assumed to cancel.

Doubly misidentified background, where the kaon and pion in the favoured mode are swapped, leads to a background that peaks at the Λ_b^0 mass in the suppressed sample. This contribution is estimated from simulation to be 0.5% in the suppressed sample, and this value is assigned as an uncertainty in R . Furthermore, the impact of $\Lambda_b^0 \rightarrow DpK^-$ decays

Table 1: Absolute uncertainties on the ratio of branching fractions, R , and CP asymmetry, A , related to the sources of systematic uncertainty studied. The statistical and total systematic uncertainties are also shown.

	R	A
Systematic uncertainties		
fit model	+0.37 -0.15	+0.000 -0.011
efficiency corrections	+0.21 -0.24	+0.010 -0.008
PID efficiency	+0.08 -0.16	+0.001 -0.002
hardware trigger efficiency	± 0.03	± 0.001
charmless background	± 0.08	
double misid. background	± 0.005	
single misid. background	± 0.001	
Λ_b^0 production asymmetry		± 0.015
p detection asymmetry		± 0.015
π detection asymmetry		± 0.005
Total systematic uncertainty	+0.43 -0.33	+0.024 -0.026
Statistical uncertainty	± 0.79	± 0.088

with subsequent $D \rightarrow K^- K^+$ or $D \rightarrow \pi^- \pi^+$ decays, when one of the D decay products is misidentified, is found to be 0.1%.

The asymmetry in Λ_b^0 and $\bar{\Lambda}_b^0$ production is expected to influence the measurement of A . The average values were measured to be $(1.92 \pm 0.35)\%$ and $(1.09 \pm 0.29)\%$ at 7 and 8 TeV centre-of-mass energies, respectively [28]. The production asymmetry is expected to decrease still further for a centre-of-mass energy of 13 TeV [29, 30]. A 1.5% systematic uncertainty is assigned. Furthermore, the detection asymmetry of the Λ_b^0 decay products is also expected to influence the measurement of A . The asymmetry in detecting protons versus antiprotons has been studied in detail [28] and does not exceed 1.5% for various values of proton momentum. The asymmetry of π^+ and π^- detection was studied in Ref. [31] and found to be less than 0.5%. These values are assigned as systematic uncertainties. Any influence of K^+ and K^- detection asymmetry is expected to cancel for the K^+ meson from the D meson and the K^- meson from the Λ_b^0 baryon.

7 Conclusion

A study of Λ_b^0 baryon decays to the $[K^\pm \pi^\mp]_D p K^-$ final state, where D indicates a superposition of D^0 and \bar{D}^0 , is reported, using a data sample corresponding to an integrated luminosity of 9 fb^{-1} collected with the LHCb detector. The suppressed $\Lambda_b^0 \rightarrow [K^+ \pi^-]_D p K^-$ decay is observed for the first time. The ratio of branching fractions for the $\Lambda_b^0 \rightarrow [K^- \pi^+]_D p K^-$ and $\Lambda_b^0 \rightarrow [K^+ \pi^-]_D p K^-$ decays, and the CP asymmetry, are measured in the full phase

space to be

$$R = 7.1 \pm 0.8 \text{ (stat.)}_{-0.3}^{+0.4} \text{ (syst.)}, A = 0.12 \pm 0.09 \text{ (stat.)}_{-0.03}^{+0.02} \text{ (syst.)}.$$

In the phase-space region $M^2(pK^-) < 5 \text{ GeV}^2/c^4$ the ratio and CP asymmetry are measured to be

$$R = 8.6 \pm 1.5 \text{ (stat.)}_{-0.3}^{+0.4} \text{ (syst.)}, \\ A = 0.01 \pm 0.16 \text{ (stat.)}_{-0.02}^{+0.03} \text{ (syst.)}.$$

Within the uncertainties, the ratio of the favoured and suppressed branching fractions is consistent with the estimate based on the relevant CKM matrix elements. The measured asymmetry values are consistent with zero, both in the full phase space and in the region where enhanced sensitivity to the CKM angle γ is expected. While the present signal yields are too low to be used to extract γ , larger samples are expected to be collected by LHCb in the coming years, and the study of this mode will contribute to the overall determination of γ .

Acknowledgements

We express our gratitude to our colleagues in the CERN accelerator departments for the excellent performance of the LHC. We thank the technical and administrative staff at the LHCb institutes. We acknowledge support from CERN and from the national agencies: CAPES, CNPq, FAPERJ and FINEP (Brazil); MOST and NSFC (China); CNRS/IN2P3 (France); BMBF, DFG and MPG (Germany); INFN (Italy); NWO (Netherlands); MNiSW and NCN (Poland); MEN/IFA (Romania); MSHE (Russia); MICINN (Spain); SNSF and SER (Switzerland); NASU (Ukraine); STFC (United Kingdom); DOE NP and NSF (USA). We acknowledge the computing resources that are provided by CERN, IN2P3 (France), KIT and DESY (Germany), INFN (Italy), SURF (Netherlands), PIC (Spain), GridPP (United Kingdom), RRCKI and Yandex LLC (Russia), CSCS (Switzerland), IFIN-HH (Romania), CBPF (Brazil), PL-GRID (Poland) and NERSC (USA). We are indebted to the communities behind the multiple open-source software packages on which we depend. Individual groups or members have received support from ARC and ARDC (Australia); AvH Foundation (Germany); EPLANET, Marie Skłodowska-Curie Actions and ERC (European Union); A*MIDEX, ANR, IPhU and Labex P2IO, and Région Auvergne-Rhône-Alpes (France); Key Research Program of Frontier Sciences of CAS, CAS PIFI, CAS CCEPP, Fundamental Research Funds for the Central Universities, and Sci. & Tech. Program of Guangzhou (China); RFBR, RSF and Yandex LLC (Russia); GVA, XuntaGal and GENCAT (Spain); the Leverhulme Trust, the Royal Society and UKRI (United Kingdom).

References

- [1] LHCb collaboration, R. Aaij *et al.*, *Study of beauty baryon decays to $D^0 p h^-$ and $\Lambda_c^+ h^-$ final states*, Phys. Rev. **D89** (2014) 032001, [arXiv:1311.4823](#).
- [2] LHCb collaboration, R. Aaij *et al.*, *Study of the $D^0 p$ amplitude in $\Lambda_b^0 \rightarrow D^0 p \pi^-$ decays*, JHEP **05** (2017) 030, [arXiv:1701.07873](#).

- [3] D. Atwood, I. Dunietz, and A. Soni, *Enhanced CP violation with $B \rightarrow KD^0(\bar{D}^0)$ modes and extraction of the CKM angle γ* , Phys. Rev. Lett. **78** (1997) 3257, arXiv:hep-ph/9612433.
- [4] D. Atwood, I. Dunietz, and A. Soni, *Improved methods for observing CP violation in $B^\pm \rightarrow KD$ and measuring the CKM phase γ* , Phys. Rev. **D63** (2001) 036005, arXiv:hep-ph/0008090.
- [5] LHCb collaboration, A. A. Alves Jr. *et al.*, *The LHCb detector at the LHC*, JINST **3** (2008) S08005.
- [6] LHCb collaboration, R. Aaij *et al.*, *LHCb detector performance*, Int. J. Mod. Phys. **A30** (2015) 1530022, arXiv:1412.6352.
- [7] R. Aaij *et al.*, *Performance of the LHCb Vertex Locator*, JINST **9** (2014) P09007, arXiv:1405.7808.
- [8] R. Arink *et al.*, *Performance of the LHCb Outer Tracker*, JINST **9** (2014) P01002, arXiv:1311.3893.
- [9] P. d'Argent *et al.*, *Improved performance of the LHCb Outer Tracker in LHC Run 2*, JINST **12** (2017) P11016, arXiv:1708.00819.
- [10] M. Adinolfi *et al.*, *Performance of the LHCb RICH detector at the LHC*, Eur. Phys. J. **C73** (2013) 2431, arXiv:1211.6759.
- [11] R. Aaij *et al.*, *The LHCb trigger and its performance in 2011*, JINST **8** (2013) P04022, arXiv:1211.3055.
- [12] T. Sjöstrand, S. Mrenna, and P. Skands, *A brief introduction to PYTHIA 8.1*, Comput. Phys. Commun. **178** (2008) 852, arXiv:0710.3820; T. Sjöstrand, S. Mrenna, and P. Skands, *PYTHIA 6.4 physics and manual*, JHEP **05** (2006) 026, arXiv:hep-ph/0603175.
- [13] I. Belyaev *et al.*, *Handling of the generation of primary events in Gauss, the LHCb simulation framework*, J. Phys. Conf. Ser. **331** (2011) 032047.
- [14] D. J. Lange, *The EvtGen particle decay simulation package*, Nucl. Instrum. Meth. **A462** (2001) 152.
- [15] N. Davidson, T. Przedzinski, and Z. Was, *PHOTOS interface in C++: Technical and physics documentation*, Comp. Phys. Comm. **199** (2016) 86, arXiv:1011.0937.
- [16] Geant4 collaboration, J. Allison *et al.*, *Geant4 developments and applications*, IEEE Trans. Nucl. Sci. **53** (2006) 270; Geant4 collaboration, S. Agostinelli *et al.*, *Geant4: A simulation toolkit*, Nucl. Instrum. Meth. **A506** (2003) 250.
- [17] M. Clemencic *et al.*, *The LHCb simulation application, Gauss: Design, evolution and experience*, J. Phys. Conf. Ser. **331** (2011) 032023.
- [18] A. Poluektov, *Kernel density estimation of a multidimensional efficiency profile*, JINST **10** (2015) P02011, arXiv:1411.5528.

- [19] Particle Data Group, P. A. Zyla *et al.*, *Review of particle physics*, Prog. Theor. Exp. Phys. **2020** (2020) 083C01.
- [20] W. D. Hulsbergen, *Decay chain fitting with a Kalman filter*, Nucl. Instrum. Meth. **A552** (2005) 566, [arXiv:physics/0503191](#).
- [21] L. Breiman, J. H. Friedman, R. A. Olshen, and C. J. Stone, *Classification and regression trees*, Wadsworth international group, Belmont, California, USA, 1984.
- [22] A. Hoecker *et al.*, *TMVA 4 — Toolkit for Multivariate Data Analysis with ROOT. Users Guide.*, [arXiv:physics/0703039](#).
- [23] W. Verkerke and D. P. Kirkby, *The RooFit toolkit for data modeling*, eConf **C0303241** (2003) MOLT007, [arXiv:physics/0306116](#).
- [24] T. Skwarnicki, *A study of the radiative cascade transitions between the Upsilon-prime and Upsilon resonances*, PhD thesis, Institute of Nuclear Physics, Krakow, 1986, DESY-F31-86-02.
- [25] M. Pivk and F. R. Le Diberder, *sPlot: A statistical tool to unfold data distributions*, Nucl. Instrum. Meth. **A555** (2005) 356, [arXiv:physics/0402083](#).
- [26] L. Anderlini *et al.*, *The PIDCalib package*, LHCb-PUB-2016-021, 2016.
- [27] R. Aaij *et al.*, *Selection and processing of calibration samples to measure the particle identification performance of the LHCb experiment in Run 2*, Eur. Phys. J. Tech. Instr. **6** (2019) 1, [arXiv:1803.00824](#).
- [28] LHCb collaboration, R. Aaij *et al.*, *Observation of a $\Lambda_b^0 - \bar{\Lambda}_b^0$ production asymmetry in proton-proton collisions at $\sqrt{s} = 7, 8$ TeV*, LHCb-PAPER-2021-016, in preparation.
- [29] E. Braaten, Y. Jia, and T. Mehen, *B production asymmetries in perturbative QCD*, Phys. Rev. **D66** (2002) 034003, [arXiv:hep-ph/0108201](#).
- [30] W. K. Lai and A. K. Leibovich, *Λ_c^+/Λ_c^- and $\Lambda_b^0/\bar{\Lambda}_b^0$ production asymmetry at the LHC from heavy quark recombination*, Phys. Rev. **D91** (2015) 054022, [arXiv:1410.2091](#).
- [31] L. Dufour, *High-precision measurements of charge asymmetries at LHCb*, PhD thesis, Groningen U., 2019.

LHCb collaboration

R. Aaij³², A.S.W. Abdelmotteleb⁵⁶, C. Abellán Beteta⁵⁰, F.J. Abudinen Gallego⁵⁶, T. Ackernley⁶⁰, B. Adeva⁴⁶, M. Adinolfi⁵⁴, H. Afsharnia⁹, C. Agapopoulou¹³, C.A. Aidala⁸⁷, S. Aiola²⁵, Z. Ajaltouni⁹, S. Akar⁶⁵, J. Albrecht¹⁵, F. Alessio⁴⁸, M. Alexander⁵⁹, A. Alfonso Alberio⁴⁵, Z. Aliouche⁶², G. Alkhazov³⁸, P. Alvarez Cartelle⁵⁵, S. Amato², J.L. Amey⁵⁴, Y. Amhis¹¹, L. An⁴⁸, L. Anderlini²², A. Andreianov³⁸, M. Andreotti²¹, F. Archilli¹⁷, A. Artamonov⁴⁴, M. Artuso⁶⁸, K. Arzymatov⁴², E. Aslanides¹⁰, M. Atzeni⁵⁰, B. Audurier¹², S. Bachmann¹⁷, M. Bachmayer⁴⁹, J.J. Back⁵⁶, P. Baladron Rodriguez⁴⁶, V. Balagura¹², W. Baldini²¹, J. Baptista Leite¹, M. Barbetti²², R.J. Barlow⁶², S. Barsuk¹¹, W. Barter⁶¹, M. Bartolini^{24,h}, F. Baryshnikov⁸³, J.M. Basels¹⁴, S. Bashir³⁴, G. Bassi²⁹, B. Batsukh⁶⁸, A. Battig¹⁵, A. Bay⁴⁹, A. Beck⁵⁶, M. Becker¹⁵, F. Bedeschi²⁹, I. Bediaga¹, A. Beiter⁶⁸, V. Belavin⁴², S. Belin²⁷, V. Bellec⁵⁰, K. Belous⁴⁴, I. Belov⁴⁰, I. Belyaev⁴¹, G. Bencivenni²³, E. Ben-Haim¹³, A. Berezhnoy⁴⁰, R. Bernet⁵⁰, D. Berninghoff¹⁷, H.C. Bernstein⁶⁸, C. Bertella⁴⁸, A. Bertolin²⁸, C. Betancourt⁵⁰, F. Betti⁴⁸, Ia. Bezshyiko⁵⁰, S. Bhasin⁵⁴, J. Bhom³⁵, L. Bian⁷³, M.S. Bieker¹⁵, S. Bifani⁵³, P. Billoir¹³, M. Birch⁶¹, F.C.R. Bishop⁵⁵, A. Bitadze⁶², A. Bizzeti^{22,k}, M. Bjørn⁶³, M.P. Blago⁴⁸, T. Blake⁵⁶, F. Blanc⁴⁹, S. Blusk⁶⁸, D. Bobulska⁵⁹, J.A. Boelhauve¹⁵, O. Boente Garcia⁴⁶, T. Boettcher⁶⁵, A. Boldyrev⁸², A. Bondar⁴³, N. Bondar^{38,48}, S. Borghi⁶², M. Borisyak⁴², M. Borsato¹⁷, J.T. Borsuk³⁵, S.A. Bouchiba⁴⁹, T.J.V. Bowcock⁶⁰, A. Boyer⁴⁸, C. Bozzi²¹, M.J. Bradley⁶¹, S. Braun⁶⁶, A. Brea Rodriguez⁴⁶, M. Brodski⁴⁸, J. Brodzicka³⁵, A. Brossa Gonzalo⁵⁶, D. Brundu²⁷, A. Buonauro⁵⁰, L. Buonincontri²⁸, A.T. Burke⁶², C. Burr⁴⁸, A. Bursche⁷², A. Butkevich³⁹, J.S. Butter³², J. Buytaert⁴⁸, W. Byczynski⁴⁸, S. Cadeddu²⁷, H. Cai⁷³, R. Calabrese^{21,f}, L. Calefice^{15,13}, L. Calero Diaz²³, S. Cali²³, R. Calladine⁵³, M. Calvi^{26,j}, M. Calvo Gomez⁸⁵, P. Camargo Magalhaes⁵⁴, P. Campana²³, A.F. Campoverde Quezada⁶, S. Capelli^{26,j}, L. Capriotti^{20,d}, A. Carbone^{20,d}, G. Carboni³¹, R. Cardinale^{24,h}, A. Cardini²⁷, I. Carli⁴, P. Carniti^{26,j}, L. Carus¹⁴, K. Carvalho Akiba³², A. Casais Vidal⁴⁶, G. Casse⁶⁰, M. Cattaneo⁴⁸, G. Cavallero⁴⁸, S. Celani⁴⁹, J. Cerasoli¹⁰, D. Cervenkov⁶³, A.J. Chadwick⁶⁰, M.G. Chapman⁵⁴, M. Charles¹³, Ph. Charpentier⁴⁸, G. Chatzikonstantinidis⁵³, C.A. Chavez Barajas⁶⁰, M. Chefdeville⁸, C. Chen³, S. Chen⁴, A. Chernov³⁵, V. Chobanova⁴⁶, S. Cholak⁴⁹, M. Chruszcz³⁵, A. Chubykin³⁸, V. Chulikov³⁸, P. Ciambrone²³, M.F. Cicala⁵⁶, X. Cid Vidal⁴⁶, G. Ciezarek⁴⁸, P.E.L. Clarke⁵⁸, M. Clemencic⁴⁸, H.V. Cliff⁵⁵, J. Closier⁴⁸, J.L. Cobble Dick⁶², V. Coco⁴⁸, J.A.B. Coelho¹¹, J. Cogan¹⁰, E. Cogneras⁹, L. Cojocariu³⁷, P. Collins⁴⁸, T. Colombo⁴⁸, L. Congedo^{19,c}, A. Contu²⁷, N. Cooke⁵³, G. Coombs⁵⁹, I. Corredoira⁴⁶, G. Corti⁴⁸, C.M. Costa Sobral⁵⁶, B. Couturier⁴⁸, D.C. Craik⁶⁴, J. Crkovač⁶⁷, M. Cruz Torres¹, R. Currie⁵⁸, C.L. Da Silva⁶⁷, S. Dadabaev⁸³, L. Dai⁷¹, E. Dall'Occo¹⁵, J. Dalseno⁴⁶, C. D'Ambrosio⁴⁸, A. Danilina⁴¹, P. d'Argent⁴⁸, J.E. Davies⁶², A. Davis⁶², O. De Aguiar Francisco⁶², K. De Bruyn⁷⁹, S. De Capua⁶², M. De Cian⁴⁹, J.M. De Miranda¹, L. De Paula², M. De Serio^{19,c}, D. De Simone⁵⁰, P. De Simone²³, J.A. de Vries⁸⁰, C.T. Dean⁶⁷, D. Decamp⁸, V. Dedu¹⁰, L. Del Buono¹³, B. Delaney⁵⁵, H.-P. Dembinski¹⁵, A. Dendek³⁴, V. Denysenko⁵⁰, D. Derkach⁸², O. Deschamps⁹, F. Desse¹¹, F. Dettori^{27,e}, B. Dey⁷⁷, A. Di Cicco²³, P. Di Nezza²³, S. Didenko⁸³, L. Dieste Maronas⁴⁶, H. Dijkstra⁴⁸, V. Dobishuk⁵², C. Dong³, A.M. Donohoe¹⁸, F. Dordei²⁷, A.C. dos Reis¹, L. Douglas⁵⁹, A. Dovbnya⁵¹, A.G. Downes⁸, M.W. Dudek³⁵, L. Dufour⁴⁸, V. Duk⁷⁸, P. Durante⁴⁸, J.M. Durham⁶⁷, D. Dutta⁶², A. Dziurda³⁵, A. Dzyuba³⁸, S. Easo⁵⁷, U. Egede⁶⁹, V. Egorychev⁴¹, S. Eidelman^{43,u}, S. Eisenhardt⁵⁸, S. Ek-In⁴⁹, L. Eklund^{59,86}, S. Ely⁶⁸, A. Ene³⁷, E. Eppele⁶⁷, S. Escher¹⁴, J. Eschle⁵⁰, S. Esen¹³, T. Evans⁴⁸, A. Falabella²⁰, J. Fan³, Y. Fan⁶, B. Fang⁷³, S. Farry⁶⁰, D. Fazzini^{26,j}, M. Féo⁴⁸, A. Fernandez Prieto⁴⁶, A.D. Fernez⁶⁶, F. Ferrari^{20,d}, L. Ferreira Lopes⁴⁹, F. Ferreira Rodrigues², S. Ferreres Sole³², M. Ferrillo⁵⁰, M. Ferro-Luzzi⁴⁸, S. Filippov³⁹, R.A. Fini¹⁹, M. Fiorini^{21,f}, M. Firlej³⁴, K.M. Fischer⁶³, D.S. Fitzgerald⁸⁷,

C. Fitzpatrick⁶², T. Fiutowski³⁴, A. Fkiaras⁴⁸, F. Fleuret¹², M. Fontana¹³, F. Fontanelli^{24,h},
 R. Forty⁴⁸, D. Foulds-Holt⁵⁵, V. Franco Lima⁶⁰, M. Franco Sevilla⁶⁶, M. Frank⁴⁸, E. Franzoso²¹,
 G. Frau¹⁷, C. Frei⁴⁸, D.A. Friday⁵⁹, J. Fu⁶, Q. Fuehring¹⁵, E. Gabriel³², A. Gallas Torreira⁴⁶,
 D. Galli^{20,d}, S. Gambetta^{58,48}, Y. Gan³, M. Gandelman², P. Gandini²⁵, Y. Gao⁵, M. Garau²⁷,
 L.M. Garcia Martin⁵⁶, P. Garcia Moreno⁴⁵, J. García Pardiñas^{26,j}, B. Garcia Plana⁴⁶,
 F.A. Garcia Rosales¹², L. Garrido⁴⁵, C. Gaspar⁴⁸, R.E. Geertsema³², D. Gerick¹⁷,
 L.L. Gerken¹⁵, E. Gersabeck⁶², M. Gersabeck⁶², T. Gershon⁵⁶, D. Gerstel¹⁰, Ph. Ghez⁸,
 L. Giambastiani²⁸, V. Gibson⁵⁵, H.K. Giemza³⁶, A.L. Gilman⁶³, M. Giovannetti^{23,p},
 A. Gioventù⁴⁶, P. Gironella Gironell⁴⁵, L. Giubega³⁷, C. Giugliano^{21,f,48}, K. Gizdov⁵⁸,
 E.L. Gkougkousis⁴⁸, V.V. Gligorov¹³, C. Göbel⁷⁰, E. Golobardes⁸⁵, D. Golubkov⁴¹,
 A. Golutvin^{61,83}, A. Gomes^{1,a}, S. Gomez Fernandez⁴⁵, F. Goncalves Abrantes⁶³, M. Goncerz³⁵,
 G. Gong³, P. Gorbounov⁴¹, I.V. Gorelov⁴⁰, C. Gotti²⁶, E. Govorkova⁴⁸, J.P. Grabowski¹⁷,
 T. Grammatico¹³, L.A. Granado Cardoso⁴⁸, E. Graugés⁴⁵, E. Graverini⁴⁹, G. Graziani²²,
 A. Grecu³⁷, L.M. Greeven³², N.A. Grieser⁴, L. Grillo⁶², S. Gromov⁸³, B.R. Gruberg Cazon⁶³,
 C. Gu³, M. Guarise²¹, M. Guittiere¹¹, P. A. Günther¹⁷, E. Gushchin³⁹, A. Guth¹⁴, Y. Guz⁴⁴,
 T. Gys⁴⁸, T. Hadavizadeh⁶⁹, G. Haefeli⁴⁹, C. Haen⁴⁸, J. Haimberger⁴⁸, T. Halewood-leagas⁶⁰,
 P.M. Hamilton⁶⁶, J.P. Hammerich⁶⁰, Q. Han⁷, X. Han¹⁷, T.H. Hancock⁶³,
 S. Hansmann-Menzemer¹⁷, N. Harnew⁶³, T. Harrison⁶⁰, C. Hasse⁴⁸, M. Hatch⁴⁸, J. He^{6,b},
 M. Hecker⁶¹, K. Heijhoff³², K. Heinicke¹⁵, A.M. Hennequin⁴⁸, K. Hennessy⁶⁰, L. Henry⁴⁸,
 J. Heuel¹⁴, A. Hicheur², D. Hill⁴⁹, M. Hilton⁶², S.E. Hollitt¹⁵, R. Hou⁷, Y. Hou⁶, J. Hu¹⁷,
 J. Hu⁷², W. Hu⁷, X. Hu³, W. Huang⁶, X. Huang⁷³, W. Hulsbergen³², R.J. Hunter⁵⁶,
 M. Hushchyn⁸², D. Hutchcroft⁶⁰, D. Hynds³², P. Ibis¹⁵, M. Idzik³⁴, D. Ilin³⁸, P. Ilten⁶⁵,
 A. Inglessi³⁸, A. Ishteev⁸³, K. Ivshin³⁸, R. Jacobsson⁴⁸, H. Jage¹⁴, S. Jakobsen⁴⁸, E. Jans³²,
 B.K. Jashal⁴⁷, A. Jawahery⁶⁶, V. Jevtic¹⁵, F. Jiang³, M. John⁶³, D. Johnson⁴⁸, C.R. Jones⁵⁵,
 T.P. Jones⁵⁶, B. Jost⁴⁸, N. Jurik⁴⁸, S.H. Kalavan Kadavath³⁴, S. Kandybei⁵¹, Y. Kang³,
 M. Karacson⁴⁸, M. Karpov⁸², F. Keizer⁴⁸, D.M. Keller⁶⁸, M. Kenzie⁵⁶, T. Ketel³³, B. Khanji¹⁵,
 A. Kharisova⁸⁴, S. Kholodenko⁴⁴, T. Kirn¹⁴, V.S. Kirsebom⁴⁹, O. Kitouni⁶⁴, S. Klaver³²,
 N. Kleijne²⁹, K. Klimaszewski³⁶, M.R. Kmiec³⁶, S. Kolliiev⁵², A. Kondybayeva⁸³,
 A. Konoplyannikov⁴¹, P. Kopciwicz³⁴, R. Kopecna¹⁷, P. Koppenburg³², M. Korolev⁴⁰,
 I. Kostiuk^{32,52}, O. Kot⁵², S. Kotriakhova^{21,38}, P. Kravchenko³⁸, L. Kravchuk³⁹,
 R.D. Krawczyk⁴⁸, M. Kreps⁵⁶, F. Kress⁶¹, S. Kretzschmar¹⁴, P. Krokovny^{43,u}, W. Krupa³⁴,
 W. Krzemien³⁶, M. Kucharczyk³⁵, V. Kudryavtsev^{43,u}, H.S. Kuindersma^{32,33}, G.J. Kunde⁶⁷,
 T. Kvaratskheliya⁴¹, D. Lacarrere⁴⁸, G. Lafferty⁶², A. Lai²⁷, A. Lampis²⁷, D. Lancierini⁵⁰,
 J.J. Lane⁶², R. Lane⁵⁴, G. Lanfranchi²³, C. Langenbruch¹⁴, J. Langer¹⁵, O. Lantwin⁸³,
 T. Latham⁵⁶, F. Lazzari^{29,q}, R. Le Gac¹⁰, S.H. Lee⁸⁷, R. Lefèvre⁹, A. Leflat⁴⁰, S. Legotin⁸³,
 O. Leroy¹⁰, T. Lesiak³⁵, B. Leverington¹⁷, H. Li⁷², P. Li¹⁷, S. Li⁷, Y. Li⁴, Y. Li⁴, Z. Li⁶⁸,
 X. Liang⁶⁸, T. Lin⁶¹, R. Lindner⁴⁸, V. Lisovskyi¹⁵, R. Litvinov²⁷, G. Liu⁷², H. Liu⁶, Q. Liu⁶,
 S. Liu⁴, A. Lobo Salvia⁴⁵, A. Loi²⁷, J. Lomba Castro⁴⁶, I. Longstaff⁵⁹, J.H. Lopes²,
 S. Lopez Solino⁴⁶, G.H. Lovell⁵⁵, Y. Lu⁴, C. Lucarelli²², D. Lucchesi^{28,l}, S. Luchuk³⁹,
 M. Lucio Martinez³², V. Lukashenko^{32,52}, Y. Luo³, A. Lupato⁶², E. Luppi^{21,f}, O. Lupton⁵⁶,
 A. Lusiani^{29,m}, X. Lyu⁶, L. Ma⁴, R. Ma⁶, S. Maccolini^{20,d}, F. Macheferri¹¹, F. Maciuc³⁷,
 V. Macko⁴⁹, P. Mackowiak¹⁵, S. Maddrell-Mander⁵⁴, O. Madejczyk³⁴, L.R. Madhan Mohan⁵⁴,
 O. Maev³⁸, A. Maevskiy⁸², D. Maisuzenko³⁸, M.W. Majewski³⁴, J.J. Malczewski³⁵, S. Malde⁶³,
 B. Malecki⁴⁸, A. Malinin⁸¹, T. Maltsev^{43,u}, H. Malygina¹⁷, G. Manca^{27,e}, G. Mancinelli¹⁰,
 D. Manuzzi^{20,d}, D. Marangotto^{25,i}, J. Maratas^{9,s}, J.F. Marchand⁸, U. Marconi²⁰, S. Mariani^{22,g},
 C. Marin Benito⁴⁸, M. Marinangeli⁴⁹, J. Marks¹⁷, A.M. Marshall⁵⁴, P.J. Marshall⁶⁰,
 G. Martelli⁷⁸, G. Martellotti³⁰, L. Martinazzoli^{48,j}, M. Martinelli^{26,j}, D. Martinez Santos⁴⁶,
 F. Martinez Vidal⁴⁷, A. Massafferri¹, M. Materok¹⁴, R. Matev⁴⁸, A. Mathad⁵⁰, Z. Mathe⁴⁸,
 V. Matiunin⁴¹, C. Matteuzzi²⁶, K.R. Mattioli⁸⁷, A. Mauri³², E. Maurice¹², J. Mauricio⁴⁵,
 M. Mazurek⁴⁸, M. McCann⁶¹, L. Mcconnell¹⁸, T.H. Mcgrath⁶², N.T. Mchugh⁵⁹, A. McNab⁶²,

R. McNulty¹⁸, J.V. Mead⁶⁰, B. Meadows⁶⁵, G. Meier¹⁵, N. Meinert⁷⁶, D. Melnychuk³⁶,
 S. Meloni^{26,j}, M. Merk^{32,80}, A. Merli^{25,i}, L. Meyer Garcia², M. Mikhasenko⁴⁸, D.A. Milanes⁷⁴,
 E. Millard⁵⁶, M. Milovanovic⁴⁸, M.-N. Minard⁸, A. Minotti^{26,j}, L. Minzoni^{21,f}, S.E. Mitchell⁵⁸,
 B. Mitreska⁶², D.S. Mitzel⁴⁸, A. Mödden¹⁵, R.A. Mohammed⁶³, R.D. Moise⁶¹, S. Mokhnenko⁸²,
 T. Mombächer⁴⁶, I.A. Monroy⁷⁴, S. Monteil⁹, M. Morandin²⁸, G. Morello²³, M.J. Morello^{29,m},
 J. Moron³⁴, A.B. Morris⁷⁵, A.G. Morris⁵⁶, R. Mountain⁶⁸, H. Mu³, F. Muheim^{58,48},
 M. Mulder⁴⁸, D. Müller⁴⁸, K. Müller⁵⁰, C.H. Murphy⁶³, D. Murray⁶², P. Muzzetto^{27,48},
 P. Naik⁵⁴, T. Nakada⁴⁹, R. Nandakumar⁵⁷, T. Nanut⁴⁹, I. Nasteva², M. Needham⁵⁸, I. Neri²¹,
 N. Neri^{25,i}, S. Neubert⁷⁵, N. Neufeld⁴⁸, R. Newcombe⁶¹, T.D. Nguyen⁴⁹, C. Nguyen-Mau^{49,v},
 E.M. Niel¹¹, S. Nieswand¹⁴, N. Nikitin⁴⁰, N.S. Nolte⁶⁴, C. Normand⁸, C. Nunez⁸⁷,
 A. Oblakowska-Mucha³⁴, V. Obraztsov⁴⁴, T. Oeser¹⁴, D.P. O'Hanlon⁵⁴, S. Okamura²¹,
 R. Oldeman^{27,e}, F. Oliva⁵⁸, M.E. Olivares⁶⁸, C.J.G. Onderwater⁷⁹, R.H. O'Neil⁵⁸,
 J.M. Otalora Goicochea², T. Ovsiannikova⁴¹, P. Owen⁵⁰, A. Oyanguren⁴⁷, K.O. Padeken⁷⁵,
 B. Pagare⁵⁶, P.R. Pais⁴⁸, T. Pajero⁶³, A. Palano¹⁹, M. Palutan²³, Y. Pan⁶², G. Panshin⁸⁴,
 A. Papanestis⁵⁷, M. Pappagallo^{19,c}, L.L. Pappalardo^{21,f}, C. Pappenheimer⁶⁵, W. Parker⁶⁶,
 C. Parkes⁶², B. Passalacqua²¹, G. Passaleva²², A. Pastore¹⁹, M. Patel⁶¹, C. Patrignani^{20,d},
 C.J. Pawley⁸⁰, A. Pearce⁴⁸, A. Pellegrino³², M. Pepe Altarelli⁴⁸, S. Perazzini²⁰, D. Pereima⁴¹,
 A. Pereiro Castro⁴⁶, P. Perret⁹, M. Petric^{59,48}, K. Petridis⁵⁴, A. Petrolini^{24,h}, A. Petrov⁸¹,
 S. Petrucci⁵⁸, M. Petruzzo²⁵, T.T.H. Pham⁶⁸, A. Philippov⁴², L. Pica^{29,m}, M. Piccini⁷⁸,
 B. Pietrzyk⁸, G. Pietrzyk⁴⁹, M. Pili⁶³, D. Pinci³⁰, F. Pisani⁴⁸, M. Pizzichemi^{26,48,j}, Resmi
 P.K¹⁰, V. Placinta³⁷, J. Plews⁵³, M. Plo Casasus⁴⁶, F. Polci¹³, M. Poli Lener²³, M. Poliakov⁶⁸,
 A. Poluektov¹⁰, N. Polukhina^{83,t}, I. Polyakov⁶⁸, E. Polycarpo², S. Ponce⁴⁸, D. Popov^{6,48},
 S. Popov⁴², S. Poslavskii⁴⁴, K. Prasanth³⁵, L. Promberger⁴⁸, C. Prouve⁴⁶, V. Pugatch⁵²,
 V. Puill¹¹, H. Pullen⁶³, G. Punzi^{29,n}, H. Qi³, W. Qian⁶, J. Qin⁶, N. Qin³, R. Quagliani⁴⁹,
 B. Quintana⁸, N.V. Raab¹⁸, R.I. Rabadan Trejo⁶, B. Rachwal³⁴, J.H. Rademacker⁵⁴,
 M. Rama²⁹, M. Ramos Pernas⁵⁶, M.S. Rangel², F. Ratnikov^{42,82}, G. Raven³³, M. Reboud⁸,
 F. Redi⁴⁹, F. Reiss⁶², C. Remon Alepuz⁴⁷, Z. Ren³, V. Renaudin⁶³, R. Ribatti²⁹, S. Ricciardi⁵⁷,
 K. Rinnert⁶⁰, P. Robbe¹¹, G. Robertson⁵⁸, A.B. Rodrigues⁴⁹, E. Rodrigues⁶⁰,
 J.A. Rodriguez Lopez⁷⁴, E.R.R. Rodriguez Rodriguez⁴⁶, A. Rollings⁶³, P. Roloff⁴⁸,
 V. Romanovskiy⁴⁴, M. Romero Lamas⁴⁶, A. Romero Vidal⁴⁶, J.D. Roth⁸⁷, M. Rotondo²³,
 M.S. Rudolph⁶⁸, T. Ruf⁴⁸, R.A. Ruiz Fernandez⁴⁶, J. Ruiz Vidal⁴⁷, A. Ryzhikov⁸², J. Ryzka³⁴,
 J.J. Saborido Silva⁴⁶, N. Sagidova³⁸, N. Sahoo⁵⁶, B. Saitta^{27,e}, M. Salomoni⁴⁸,
 C. Sanchez Gras³², R. Santacesaria³⁰, C. Santamarina Rios⁴⁶, M. Santimaria²³,
 E. Santovetti^{31,p}, D. Saranin⁸³, G. Sarpis¹⁴, M. Sarpis⁷⁵, A. Sarti³⁰, C. Satriano^{30,o}, A. Satta³¹,
 M. Saur¹⁵, D. Savrina^{41,40}, H. Sazak⁹, L.G. Scantlebury Smead⁶³, A. Scarabotto¹³, S. Schael¹⁴,
 S. Scherl⁶⁰, M. Schiller⁵⁹, H. Schindler⁴⁸, M. Schmelling¹⁶, B. Schmidt⁴⁸, S. Schmitt¹⁴,
 O. Schneider⁴⁹, A. Schopper⁴⁸, M. Schubiger³², S. Schulte⁴⁹, M.H. Schune¹¹, R. Schwemmer⁴⁸,
 B. Sciascia^{23,48}, S. Sellam⁴⁶, A. Semennikov⁴¹, M. Senghi Soares³³, A. Sergi^{24,h}, N. Serra⁵⁰,
 L. Sestini²⁸, A. Seuthe¹⁵, Y. Shang⁵, D.M. Shangase⁸⁷, M. Shapkin⁴⁴, I. Shchemerov⁸³,
 L. Shchutka⁴⁹, T. Shears⁶⁰, L. Shekhtman^{43,u}, Z. Shen⁵, V. Shevchenko⁸¹, E.B. Shields^{26,j},
 Y. Shimizu¹¹, E. Shmanin⁸³, J.D. Shupperd⁶⁸, B.G. Siddi²¹, R. Silva Coutinho⁵⁰, G. Simi²⁸,
 S. Simone^{19,c}, E. Sirks⁴⁸, N. Skidmore⁶², T. Skwarnicki⁶⁸, M.W. Slater⁵³, I. Slazyk^{21,f},
 J.C. Smallwood⁶³, J.G. Smeaton⁵⁵, A. Smetkina⁴¹, E. Smith⁵⁰, M. Smith⁶¹, A. Snoch³²,
 M. Soares²⁰, L. Soares Lavra⁹, M.D. Sokoloff⁶⁵, F.J.P. Soler⁵⁹, A. Solovev³⁸, I. Solovyev³⁸,
 F.L. Souza De Almeida², B. Souza De Paula², B. Spaan¹⁵, E. Spadaro Norella^{25,i}, P. Spradlin⁵⁹,
 F. Stagni⁴⁸, M. Stahl⁶⁵, S. Stahl⁴⁸, S. Stanislaus⁶³, O. Steinkamp^{50,83}, O. Stenyakin⁴⁴,
 H. Stevens¹⁵, S. Stone⁶⁸, M. Straticiu³⁷, D. Strelakina⁸³, F. Suljik⁶³, J. Sun²⁷, L. Sun⁷³,
 Y. Sun⁶⁶, P. Svihra⁶², P.N. Swallow⁵³, K. Swientek³⁴, A. Szabelski³⁶, T. Szumlak³⁴,
 M. Szymanski⁴⁸, S. Taneja⁶², A.R. Tanner⁵⁴, M.D. Tat⁶³, A. Terentev⁸³, F. Teubert⁴⁸,
 E. Thomas⁴⁸, D.J.D. Thompson⁵³, K.A. Thomson⁶⁰, V. Tisserand⁹, S. T'Jampens⁸, M. Tobin⁴,

L. Tomassetti^{21,f}, X. Tong⁵, D. Torres Machado¹, D.Y. Tou¹³, M.T. Tran⁴⁹, E. Trifonova⁸³, C. Trippel⁴⁹, G. Tuci⁶, A. Tully⁴⁹, N. Tuning^{32,48}, A. Ukleja³⁶, D.J. Unverzagt¹⁷, E. Ursov⁸³, A. Usachov³², A. Ustyuzhanin^{42,82}, U. Uwer¹⁷, A. Vagner⁸⁴, V. Vagnoni²⁰, A. Valassi⁴⁸, G. Valenti²⁰, N. Valls Canudas⁸⁵, M. van Beuzekom³², M. Van Dijk⁴⁹, E. van Herwijnen⁸³, C.B. Van Hulse¹⁸, M. van Veghel⁷⁹, R. Vazquez Gomez⁴⁵, P. Vazquez Regueiro⁴⁶, C. Vázquez Sierra⁴⁸, S. Vecchi²¹, J.J. Velthuis⁵⁴, M. Veltri^{22,r}, A. Venkateswaran⁶⁸, M. Veronesi³², M. Vesterinen⁵⁶, D. Vieira⁶⁵, M. Vieites Diaz⁴⁹, H. Viemann⁷⁶, X. Vilasis-Cardona⁸⁵, E. Vilella Figueras⁶⁰, A. Villa²⁰, P. Vincent¹³, F.C. Volle¹¹, D. Vom Bruch¹⁰, A. Vorobyev³⁸, V. Vorobyev^{43,u}, N. Voropaev³⁸, K. Vos⁸⁰, R. Waldi¹⁷, J. Walsh²⁹, C. Wang¹⁷, J. Wang⁵, J. Wang⁴, J. Wang³, J. Wang⁷³, M. Wang³, R. Wang⁵⁴, Y. Wang⁷, Z. Wang⁵⁰, Z. Wang³, Z. Wang⁶, J.A. Ward⁵⁶, N.K. Watson⁵³, S.G. Weber¹³, D. Websdale⁶¹, C. Weisser⁶⁴, B.D.C. Westhenry⁵⁴, D.J. White⁶², M. Whitehead⁵⁴, A.R. Wiederhold⁵⁶, D. Wiedner¹⁵, G. Wilkinson⁶³, M. Wilkinson⁶⁸, I. Williams⁵⁵, M. Williams⁶⁴, M.R.J. Williams⁵⁸, F.F. Wilson⁵⁷, W. Wislicki³⁶, M. Witek³⁵, L. Witola¹⁷, G. Wormser¹¹, S.A. Wotton⁵⁵, H. Wu⁶⁸, K. Wyllie⁴⁸, Z. Xiang⁶, D. Xiao⁷, Y. Xie⁷, A. Xu⁵, J. Xu⁶, L. Xu³, M. Xu⁷, Q. Xu⁶, Z. Xu⁵, Z. Xu⁶, D. Yang³, S. Yang⁶, Y. Yang⁶, Z. Yang⁵, Z. Yang⁶⁶, Y. Yao⁶⁸, L.E. Yeomans⁶⁰, H. Yin⁷, J. Yu⁷¹, X. Yuan⁶⁸, O. Yushchenko⁴⁴, E. Zaffaroni⁴⁹, M. Zavertyaev^{16,t}, M. Zdybal³⁵, O. Zenaiev⁴⁸, M. Zeng³, D. Zhang⁷, L. Zhang³, S. Zhang⁷¹, S. Zhang⁵, Y. Zhang⁵, Y. Zhang⁶³, A. Zharkova⁸³, A. Zhelezov¹⁷, Y. Zheng⁶, T. Zhou⁵, X. Zhou⁶, Y. Zhou⁶, V. Zhovkovska¹¹, X. Zhu³, X. Zhu⁷, Z. Zhu⁶, V. Zhukov^{14,40}, J.B. Zonneveld⁵⁸, Q. Zou⁴, S. Zucchelli^{20,d}, D. Zuliani²⁸, G. Zunica⁶².

¹Centro Brasileiro de Pesquisas Físicas (CBPF), Rio de Janeiro, Brazil

²Universidade Federal do Rio de Janeiro (UFRJ), Rio de Janeiro, Brazil

³Center for High Energy Physics, Tsinghua University, Beijing, China

⁴Institute Of High Energy Physics (IHEP), Beijing, China

⁵School of Physics State Key Laboratory of Nuclear Physics and Technology, Peking University, Beijing, China

⁶University of Chinese Academy of Sciences, Beijing, China

⁷Institute of Particle Physics, Central China Normal University, Wuhan, Hubei, China

⁸Univ. Savoie Mont Blanc, CNRS, IN2P3-LAPP, Annecy, France

⁹Université Clermont Auvergne, CNRS/IN2P3, LPC, Clermont-Ferrand, France

¹⁰Aix Marseille Univ, CNRS/IN2P3, CPPM, Marseille, France

¹¹Université Paris-Saclay, CNRS/IN2P3, IJCLab, Orsay, France

¹²Laboratoire Leprince-Ringuet, CNRS/IN2P3, Ecole Polytechnique, Institut Polytechnique de Paris, Palaiseau, France

¹³LPNHE, Sorbonne Université, Paris Diderot Sorbonne Paris Cité, CNRS/IN2P3, Paris, France

¹⁴I. Physikalisches Institut, RWTH Aachen University, Aachen, Germany

¹⁵Fakultät Physik, Technische Universität Dortmund, Dortmund, Germany

¹⁶Max-Planck-Institut für Kernphysik (MPIK), Heidelberg, Germany

¹⁷Physikalisches Institut, Ruprecht-Karls-Universität Heidelberg, Heidelberg, Germany

¹⁸School of Physics, University College Dublin, Dublin, Ireland

¹⁹INFN Sezione di Bari, Bari, Italy

²⁰INFN Sezione di Bologna, Bologna, Italy

²¹INFN Sezione di Ferrara, Ferrara, Italy

²²INFN Sezione di Firenze, Firenze, Italy

²³INFN Laboratori Nazionali di Frascati, Frascati, Italy

²⁴INFN Sezione di Genova, Genova, Italy

²⁵INFN Sezione di Milano, Milano, Italy

²⁶INFN Sezione di Milano-Bicocca, Milano, Italy

²⁷INFN Sezione di Cagliari, Monserrato, Italy

²⁸Università degli Studi di Padova, Università e INFN, Padova, Padova, Italy

²⁹INFN Sezione di Pisa, Pisa, Italy

³⁰INFN Sezione di Roma La Sapienza, Roma, Italy

- ³¹ *INFN Sezione di Roma Tor Vergata, Roma, Italy*
- ³² *Nikhef National Institute for Subatomic Physics, Amsterdam, Netherlands*
- ³³ *Nikhef National Institute for Subatomic Physics and VU University Amsterdam, Amsterdam, Netherlands*
- ³⁴ *AGH - University of Science and Technology, Faculty of Physics and Applied Computer Science, Kraków, Poland*
- ³⁵ *Henryk Niewodniczanski Institute of Nuclear Physics Polish Academy of Sciences, Kraków, Poland*
- ³⁶ *National Center for Nuclear Research (NCBJ), Warsaw, Poland*
- ³⁷ *Horia Hulubei National Institute of Physics and Nuclear Engineering, Bucharest-Magurele, Romania*
- ³⁸ *Petersburg Nuclear Physics Institute NRC Kurchatov Institute (PNPI NRC KI), Gatchina, Russia*
- ³⁹ *Institute for Nuclear Research of the Russian Academy of Sciences (INR RAS), Moscow, Russia*
- ⁴⁰ *Institute of Nuclear Physics, Moscow State University (SINP MSU), Moscow, Russia*
- ⁴¹ *Institute of Theoretical and Experimental Physics NRC Kurchatov Institute (ITEP NRC KI), Moscow, Russia*
- ⁴² *Yandex School of Data Analysis, Moscow, Russia*
- ⁴³ *Budker Institute of Nuclear Physics (SB RAS), Novosibirsk, Russia*
- ⁴⁴ *Institute for High Energy Physics NRC Kurchatov Institute (IHEP NRC KI), Protvino, Russia, Protvino, Russia*
- ⁴⁵ *ICCUB, Universitat de Barcelona, Barcelona, Spain*
- ⁴⁶ *Instituto Galego de Física de Altas Enerxías (IGFAE), Universidade de Santiago de Compostela, Santiago de Compostela, Spain*
- ⁴⁷ *Instituto de Física Corpuscular, Centro Mixto Universidad de Valencia - CSIC, Valencia, Spain*
- ⁴⁸ *European Organization for Nuclear Research (CERN), Geneva, Switzerland*
- ⁴⁹ *Institute of Physics, Ecole Polytechnique Fédérale de Lausanne (EPFL), Lausanne, Switzerland*
- ⁵⁰ *Physik-Institut, Universität Zürich, Zürich, Switzerland*
- ⁵¹ *NSC Kharkiv Institute of Physics and Technology (NSC KIPT), Kharkiv, Ukraine*
- ⁵² *Institute for Nuclear Research of the National Academy of Sciences (KINR), Kyiv, Ukraine*
- ⁵³ *University of Birmingham, Birmingham, United Kingdom*
- ⁵⁴ *H.H. Wills Physics Laboratory, University of Bristol, Bristol, United Kingdom*
- ⁵⁵ *Cavendish Laboratory, University of Cambridge, Cambridge, United Kingdom*
- ⁵⁶ *Department of Physics, University of Warwick, Coventry, United Kingdom*
- ⁵⁷ *STFC Rutherford Appleton Laboratory, Didcot, United Kingdom*
- ⁵⁸ *School of Physics and Astronomy, University of Edinburgh, Edinburgh, United Kingdom*
- ⁵⁹ *School of Physics and Astronomy, University of Glasgow, Glasgow, United Kingdom*
- ⁶⁰ *Oliver Lodge Laboratory, University of Liverpool, Liverpool, United Kingdom*
- ⁶¹ *Imperial College London, London, United Kingdom*
- ⁶² *Department of Physics and Astronomy, University of Manchester, Manchester, United Kingdom*
- ⁶³ *Department of Physics, University of Oxford, Oxford, United Kingdom*
- ⁶⁴ *Massachusetts Institute of Technology, Cambridge, MA, United States*
- ⁶⁵ *University of Cincinnati, Cincinnati, OH, United States*
- ⁶⁶ *University of Maryland, College Park, MD, United States*
- ⁶⁷ *Los Alamos National Laboratory (LANL), Los Alamos, United States*
- ⁶⁸ *Syracuse University, Syracuse, NY, United States*
- ⁶⁹ *School of Physics and Astronomy, Monash University, Melbourne, Australia, associated to ⁵⁶*
- ⁷⁰ *Pontifícia Universidade Católica do Rio de Janeiro (PUC-Rio), Rio de Janeiro, Brazil, associated to ²*
- ⁷¹ *Physics and Micro Electronic College, Hunan University, Changsha City, China, associated to ⁷*
- ⁷² *Guangdong Provincial Key Laboratory of Nuclear Science, Guangdong-Hong Kong Joint Laboratory of Quantum Matter, Institute of Quantum Matter, South China Normal University, Guangzhou, China, associated to ³*
- ⁷³ *School of Physics and Technology, Wuhan University, Wuhan, China, associated to ³*
- ⁷⁴ *Departamento de Física, Universidad Nacional de Colombia, Bogota, Colombia, associated to ¹³*
- ⁷⁵ *Universität Bonn - Helmholtz-Institut für Strahlen und Kernphysik, Bonn, Germany, associated to ¹⁷*
- ⁷⁶ *Institut für Physik, Universität Rostock, Rostock, Germany, associated to ¹⁷*
- ⁷⁷ *Eotvos Lorand University, Budapest, Hungary, associated to ⁴⁸*
- ⁷⁸ *INFN Sezione di Perugia, Perugia, Italy, associated to ²¹*
- ⁷⁹ *Van Swinderen Institute, University of Groningen, Groningen, Netherlands, associated to ³²*

- ⁸⁰ *Universiteit Maastricht, Maastricht, Netherlands, associated to* ³²
⁸¹ *National Research Centre Kurchatov Institute, Moscow, Russia, associated to* ⁴¹
⁸² *National Research University Higher School of Economics, Moscow, Russia, associated to* ⁴²
⁸³ *National University of Science and Technology "MISIS", Moscow, Russia, associated to* ⁴¹
⁸⁴ *National Research Tomsk Polytechnic University, Tomsk, Russia, associated to* ⁴¹
⁸⁵ *DS4DS, La Salle, Universitat Ramon Llull, Barcelona, Spain, associated to* ⁴⁵
⁸⁶ *Department of Physics and Astronomy, Uppsala University, Uppsala, Sweden, associated to* ⁵⁹
⁸⁷ *University of Michigan, Ann Arbor, United States, associated to* ⁶⁸

^a *Universidade Federal do Triângulo Mineiro (UFMT), Uberaba-MG, Brazil*

^b *Hangzhou Institute for Advanced Study, UCAS, Hangzhou, China*

^c *Università di Bari, Bari, Italy*

^d *Università di Bologna, Bologna, Italy*

^e *Università di Cagliari, Cagliari, Italy*

^f *Università di Ferrara, Ferrara, Italy*

^g *Università di Firenze, Firenze, Italy*

^h *Università di Genova, Genova, Italy*

ⁱ *Università degli Studi di Milano, Milano, Italy*

^j *Università di Milano Bicocca, Milano, Italy*

^k *Università di Modena e Reggio Emilia, Modena, Italy*

^l *Università di Padova, Padova, Italy*

^m *Scuola Normale Superiore, Pisa, Italy*

ⁿ *Università di Pisa, Pisa, Italy*

^o *Università della Basilicata, Potenza, Italy*

^p *Università di Roma Tor Vergata, Roma, Italy*

^q *Università di Siena, Siena, Italy*

^r *Università di Urbino, Urbino, Italy*

^s *MSU - Iligan Institute of Technology (MSU-IIT), Iligan, Philippines*

^t *P.N. Lebedev Physical Institute, Russian Academy of Science (LPI RAS), Moscow, Russia*

^u *Novosibirsk State University, Novosibirsk, Russia*

^v *Hanoi University of Science, Hanoi, Vietnam*